Orexin-A represses satiety-inducing POMC neurons and contributes to obesity via stimulation of endocannabinoid signaling

Giovanna Morello[a,b,1], Roberta Imperatore[a,1], Letizia Palomba[c], Carmine Finelli[d], Giuseppe Labruna[e], Fabrizio Pasanisi[d], Lucia Sacchetti[f], Lorena Buono[a,g], Fabiana Piscitelli[a], Pierangelo Orlando[h], Vincenzo Di Marzo[a], and Luigia Cristino[a,2]

[a]Institute of Biomolecular Chemistry, National Research Council, 80078 Pozzuoli, Italy; [b]Department of Neurological and Movement Sciences, University of Verona, 37137 Verona, Italy; [c]Department of Biomolecular Sciences, University of Urbino "Carlo Bo," 61029 Urbino, Italy; [d]Interuniversity Center for Research and Study of Obesity, Department of Clinical and Experimental Medicine, Federico II University Hospital, 80131 Naples, Italy; [e]Istituto di Ricovero e Cura a Carattere Scientifico, Institute of Diagnostic and Nuclear Research, 80131 Naples, Italy; [f]Centro di Ingegneria Genetica–Advanced Biotechnology (Società Cooperativa a Responsabilità Limitata), 80131 Naples, Italy; [g]Centro de Biología Molecular "Severo Ochoa," Consejo Superior de Investigaciones Científicas–Universidad Autónoma de Madrid, 28049 Cantoblanco, Spain; and [h]Institute of Protein Biochemistry, National Research Council, 80131 Naples, Italy

Edited by Tamas L. Horvath, Yale University School of Medicine, New Haven, CT, and accepted by the Editorial Board March 8, 2016 (received for review October 28, 2015)

In the hypothalamic arcuate nucleus (ARC), proopiomelanocortin (POMC) neurons and the POMC-derived peptide α–melanocyte-stimulating hormone (α-MSH) promote satiety. POMC neurons receive orexin-A (OX-A)-expressing inputs and express both OX-A receptor type 1 (OX-1R) and cannabinoid receptor type 1 (CB_1R) on the plasma membrane. OX-A is crucial for the control of wakefulness and energy homeostasis and promotes, in OX-1R–expressing cells, the biosynthesis of the endogenous counterpart of marijuana's psychotropic and appetite-inducing component Δ^9-tetrahydrocannabinol, i.e., the endocannabinoid 2-arachidonoylglycerol (2-AG), which acts at CB_1R. We report that OX-A/OX-1R signaling at POMC neurons promotes 2-AG biosynthesis, hyperphagia, and weight gain by blunting α-MSH production via CB_1R-induced and extracellular-signal-regulated kinase 1/2 activation- and STAT3 inhibition-mediated suppression of *Pomc* gene transcription. Because the systemic pharmacological blockade of OX-1R by SB334867 caused anorectic effects by reducing food intake and body weight, our results unravel a previously unsuspected role for OX-A in endocannabinoid-mediated promotion of appetite by combining OX-induced alertness with food seeking. Notably, increased OX-A trafficking was found in the fibers projecting to the ARC of obese mice (*ob/ob* and high-fat diet fed) concurrently with elevation of OX-A release in the cerebrospinal fluid and blood of mice. Furthermore, a negative correlation between OX-A and α-MSH serum levels was found in obese mice as well as in human obese subjects (body mass index > 40), in combination with elevation of alanine aminotransferase and γ-glutamyl transferase, two markers of fatty liver disease. These alterations were counteracted by antagonism of OX-1R, thus providing the basis for a therapeutic treatment of these diseases.

hypocretin-1 | cannabinoid type 1 receptor | 2-arachidonoylglycerol | α–melanocyte-stimulating hormone | hypothalamus

Emerging anatomical, biochemical, and pharmacological evidence supports a functional interaction between endocannabinoids and orexin-A (OX-A) (also known as hypocretin-1) in the hypothalamic regulation of appetite, energy expenditure, and metabolism (1). In hypothalamic neurons, the endocannabinoid 2-arachidonylglycerol (2-AG) is under the negative control of leptin (2) and acts through the cannabinoid receptor type 1 (CB_1R) to promote appetite by activating several intracellular pathways, including mitogen-activated protein kinases of the extracellular-signal-regulated kinase (ERK) family (3). OX-A is an orexigenic neuropeptide expressed by neurons of the lateral hypothalamus (LH), which acts through the OX-A receptor type 1 (OX-1R) (4). Activation of OX-1R by OX-A signaling has been found to affect CB_1R function by stimulating 2-AG biosynthesis via the phospholipase C/diacylglycerol lipase α (PLC/DAGL) pathway (5) and by enhancing ERK1/2 phosphorylation and activity in cells expressing both OX-1R and CB_1R (6, 7). Proopiomelanocortin (POMC)-containing neurons represent the master subset of hypothalamic anorexigenic neurons, being the source of the α–melanocyte-stimulating hormone (α-MSH), which suppresses feeding and/or stimulates energy expenditure (8–10). Ablation of POMC neurons or loss of α-MSH causes obesity (11, 12), whereas mutations of the melanocortin 4 receptors (MC4R) for α-MSH are associated with human obesity (13). POMC neurons receive inhibitory OX-A inputs that, during rest and sleep periods, suppress hunger by enhancing firing (14–16), whereas OX-A expression in the LH is inhibited by α-MSH (17). Notably, marijuana's psychotropic and appetite-inducing component, Δ^9-tetrahydrocannabinol (THC), acts at a population of CB_1Rs located in the mitochondria of POMC neurons without affecting α-MSH production (18). Furthermore, the CB_1R antagonist rimonabant attenuates the orexigenic actions of OX-A (19). This evidence suggests the existence of an OX-A–controlled hypothalamic loop of potential evolutionary

Significance

Both evolutionarily and functionally, wakefulness requires, and is accompanied by, food search and intake for survival. From the molecular perspective, the neuropeptide orexin-A (OX-A) promotes wakefulness, α–melanocyte-stimulating hormone (α-MSH) promotes satiety, and the endocannabinoid 2-arachidonoylglycerol (2-AG) promotes appetite. In the cerebrospinal fluid of obese mice and in the plasma of human obese subjects, we found an inverse correlation between OX-A and α-MSH levels, which led us to uncover the role of OX-A in promoting hyperphagia by enhancing 2-AG levels and subsequently activating CB_1 receptor-mediated down-regulation of POMC synthesis and α-MSH release. Pharmacological inhibition of OX-A receptor type 1 counteracted the impairment of α-MSH signaling and the associated hyperphagia, obesity, and steatosis, thus providing a potential therapy for these pathological conditions.

Author contributions: L.P., F. Pasanisi., L.S., and L.C. designed research; G.M., R.I., L.P., C.F., G.L., F. Pasanisi, L.B., F. Piscitelli, and P.O. performed research; L.S. and P.O. contributed new reagents/analytic tools; G.M., R.I., L.P., C.F., G.L., F. Pasanisi, L.S., L.B., F. Piscitelli, P.O., V.D., and L.C. analyzed data; and V.D. and L.C. wrote the paper.

The authors declare no conflict of interest.

This article is a PNAS Direct Submission. T.L.H. is a guest editor invited by the Editorial Board.

[1]G.M. and R.I. contributed equally to this work.

[2]To whom correspondence should be addressed. Email: luigia.cristino@icb.cnr.it.

This article contains supporting information online at www.pnas.org/lookup/suppl/doi:10.1073/pnas.1521304113/-/DCSupplemental.

relevance as it would ensure that alertness is accompanied by food seeking. However, the molecular mechanism(s) underlying this pathway remain(s), surprisingly, still unexplored. We have previously reported that leptin signaling deficiency in obese mice [both in leptin-knockout *ob*/*ob* and high-fat diet (HFD)-fed mice] causes elevation of 2-AG production and synaptic rewiring to OX-A neurons with consequent increase of OX-A release to target areas, including the arcuate nucleus (ARC) (20). Here, we provide anatomical, molecular, biochemical, and pharmacological evidence that OX-A/OX-1R signaling at POMC neurons in the ARC reduces POMC and α-MSH production via an autocrine, transcriptional endocannabinoid/ERK/STAT3-mediated mechanism in sated mice. We further analyzed the potential impact of this pathway on food intake, body weight, and fatty liver disease in obese mice and human subjects.

Results

OX-A Expression Is Increased in the ARC of Obese Mice. Hypothalamic leptin signal deficiency in *ob*/*ob* and HFD obese mice is accompanied by increased OX-A immunoreactivity in fibers projecting to the ARC and enhanced cFos expression in OX-A neurons of LH (Fig. 1 *A* and *B*). CB_1Rs are involved in mediating these effects because 1-h treatment with the CB_1R inverse agonist AM251 (10 mg/kg, i.p.) reduced cFos expression in OX-A neurons and OX-A immunoreactivity in fibers to the ARC in both models (Fig. 1 *A* and *B*), whereas leptin (5 mg/kg, 2 h i.p.) was effective in *ob*/*ob*, but not in HFD mice (Fig. 1*A* and *SI Appendix*, Fig. S1*A*), because of hypothalamic leptin insensitivity as previously shown in this latter model (20). Notably, OX-A immunodensity of ARC fibers matches with the increase of OX-A release in the cerebrospinal fluid (CSF) of obese mice (Fig. 1*C*).

OX-A Drives 2-AG Biosynthesis in the ARC. The levels of 2-AG were increased in the ARC of OX-A–injected lean, *ob*/*ob* vehicle-injected, or HFD vehicle-injected mice in comparison with vehicle-injected lean mice (Fig. 1*D*). This increase was counteracted by leptin in *ob*/*ob* mice (5 mg/kg; i.p., 1 h; *SI Appendix*, Fig. S1*A*) and, in both models, by (*i*) antagonism of OX-1R (SB334867, 30 mg/kg; i.p., 1 h; Fig. 1*D*) and (*ii*) inhibition of the 2-AG biosynthetic enzyme, DAGLα (O-7460; 12 mg/kg; i.p., 1 h; *SI Appendix*, Fig. S1*A*). Because immunolabeling of DAGLα was concentrated in the somata of POMC neurons and in the neuropil of ARC (*SI Appendix*, Fig. S1*B*), the ARC primary neurons or isolated primary POMC-eGFP neurons cultured from the ARC POMC-eGFP heterozygote transgenic mice were tested as a source of 2-AG. Similar to the in vivo situation, OX-A was able to strongly elevate 2-AG levels in primary neurons in a manner sensitive to SB334867 and O-7460 (*SI Appendix*, Table S1). Moreover, a reduction of phosphatidylinositol 4,5-bisphosphate [PI(4,5)P_2] levels, reversed by SB334867, was observed in OX-A–treated

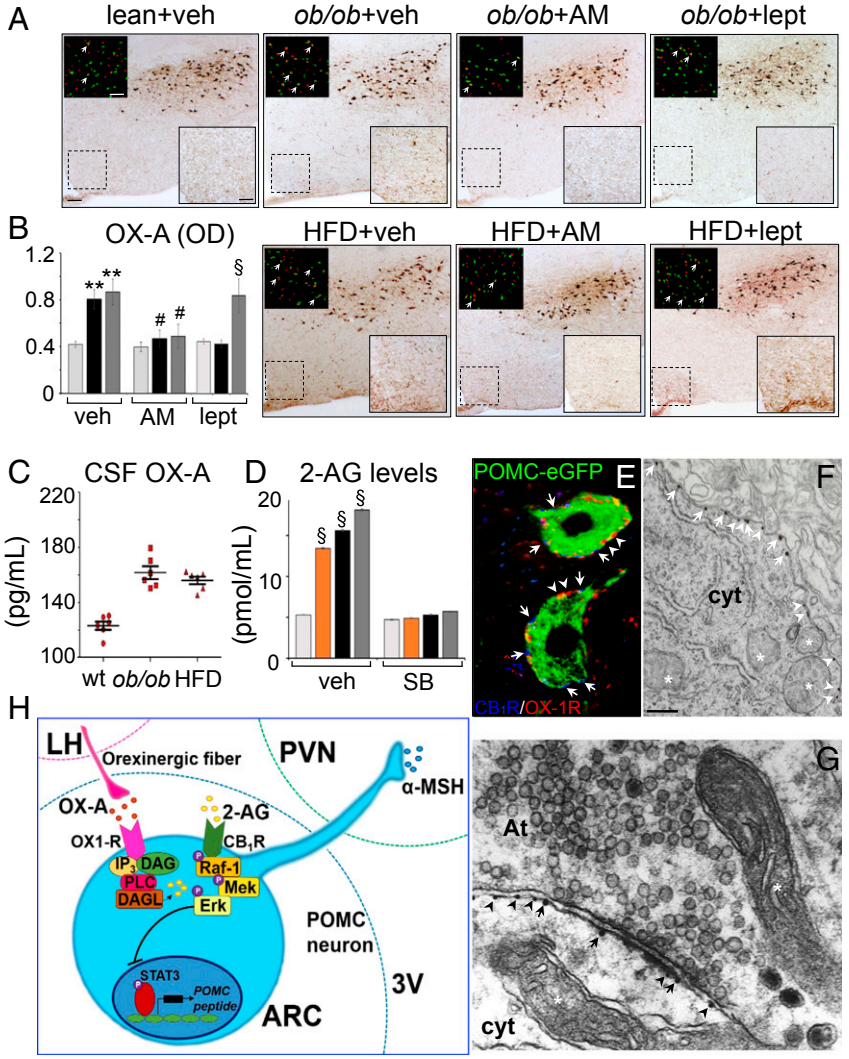

Fig. 1. OX-A increases in the fibers of the ARC of obese mice enhancing 2-AG biosynthesis. (*A*) Representative coronal sections of similar rostrocaudal position of the LH and ARC (scale bar: 100 μm) showing labeled fibers and puncta in the ARC (high magnification of the respective boxed area; scale bar: 50 μm) and cFOS/OX-A costaining in the LH (*Insets*; scale bar: 100 μm). (*B*) Bar graphs of OX-A peroxidase-based optical density (OD, arbitrary units) in the ARC of lean (light gray bars), *ob*/*ob* (black bars), or HFD (dark gray bars) mice. $^{**}P < 0.005$ vs. vehicle-injected lean mice; $^{\#}P < 0.05$ vs. AM251-injected mice. $^{\S}P < 0.005$ vs. leptin-injected lean mice. (*C*) OX-A levels in the CSF. (*D*) 2-AG levels in the ARC of lean (light gray bars), OX-A–injected lean (orange bars), *ob*/*ob* (black bars), or HFD (dark gray bars) mice reversed by SB334867 treatment. $^{\S}P < 0.0005$ vs. vehicle-injected lean mice. (*E* and *F*) CB_1R and OX-1R immuno-coexpression in POMC neurons. CB_1R and OX-1R electron microscopy immunogold detection at the plasma membrane (*F*) and postsynaptic side (*G*) of POMC neurons. CB_1R (arrows) and OX-1R (arrowheads). At, axon terminal; cyt, cytoplasm; mitochondria are indicated by the asterisk [scale bar: 10 μm (*E*); 0.2 μm (*F* and *G*)]. Data are means ± SEM; $n = 6$ mice per group fed ad libitum. Statistical analysis was performed by two-way ANOVA followed by the Bonferroni post hoc test. (*H*) Scheme of the molecular pathway underlying CB_1R activation, and subsequent transcriptional blockade of POMC expression, via OX-A–induced 2-AG production. 3V, third ventricle; DAG, diacylglycerol; IP_3, inositol triphosphate; MEK, mitogen-activated protein kinase; OX1-R, orexin receptor type-1; PVN, paraventricular nucleus; Raf-1, protein kinase.

POMC-eGFP primary neurons [untreated: 108 ± 8.5; OX-A: 60 ± 7.2; OX-A plus SB334867: 90 ± 8.1; SB334867: 95 ± 9.4; $PI(4,5)P_2$ levels are expressed as picomoles per 10,000 cells ± SEM], thus confirming that OX-A potentiates endocannabinoid signaling via OX-1R–dependent activation of the PLC/DAGLα-dependent regulatory pathway.

CB_1R and OX-1R Are Coexpressed in POMC Neurons of the ARC. Because CB_1R has been found in a large population of POMC neurons (18) and our evidence suggests that OX-A might act as an enhancer of CB_1R signaling by promoting 2-AG synthesis, both in the ARC and in isolated POMC neurons, we analyzed whether CB_1R and OX-1R are colocalized in these neurons. By confocal and high-resolution electron microscopy, we documented in the ARC the expression of CB_1R in the plasma membrane of 73.4% (144 of 196) of POMC neurons, where it was coexpressed with OX-1R in 86.8% (125 of 144) of CB_1R/POMC neurons (Fig. 1 *E* and *F*). By electron microscopy immunogold labeling, we revealed CB_1R expression at the postsynaptic side (i.e., postsynaptic density of boutons) in 22.4% (22 of 98) of POMC neurons (Fig. 1*G*). Furthermore, CB_1R was localized rarely at the presynaptic site of axosomatic synapses apposed to POMC somata, in agreement with Hentges (21); rarely at mitochondrial compartments of POMC neurons, in agreement with Bénard et al. (22) who, in the hippocampus, revealed that ∼15% of the CA1 neuronal total CB_1R protein was localized to mitochondria. Notably, the frequency of CB_1R and OX-1R metal particle distribution per micrometer of cell membrane did not change between obese (OX-1R, $n = 4.3 \pm 0.6$; CB_1R, $n = 3.1 \pm 0.5$) and lean (OX-1R, $n = 4.7 \pm 0.4$; CB_1R, $n = 3.3 \pm 0.4$) mice.

OX-A–Induced Hyperphagia in Mice Relies on Inhibition of Neuronal POMC Expression and α-MSH Production via CB_1R Activation and ERK1/2-Mediated $STAT3^{Ser727}$ Phosphorylation. It is known that 2-AG acts through CB_1R to promote appetite via potentiation of ERK1/2 activity, which is also the main downstream target for OX-1R (23–27). We found a strong increase of ERK1/2 phosphorylation/activation (i.e., of $pERK1/2^{Thr202/Tyr204}$ levels) in POMC neurons of lean mice following injection of OX-A, and in POMC neurons of *ob*/*ob* and in HFD mice characterized by elevated OX-A signaling. This effect was (*i*) antagonized by the CB_1R inverse agonist AM251, and hence possibly due to OX-A–induced 2-AG biosynthesis and CB_1R-mediated ERK1/2 phosphorylation; (*ii*) followed by enhancement of STAT3 phosphorylation at Ser727 without significant change in Tyr705 phosphorylation (Fig. 2*A* and *SI Appendix*, Fig. S2); and (*iii*) followed by down-regulation of *Pomc* gene transcription (Fig. 2*B* and *SI Appendix*, Fig. S3 *A*–*C*). These effects were also counteracted by the ERK1/2 inhibitor, PD98059, and SB334867 (Fig. 2 *A* and *B*, and *SI Appendix*, Figs. S2 and S3 *A*–*C*). Interestingly, basal *Pomc* mRNA levels of ad libitum fed *ob*/*ob* and HFD mice were decreased by 80–90% in comparison with ad libitum fed lean mice (*SI Appendix*, Fig. S3*A*). This reduction was fully reversed by SB334867 in both *ob*/*ob* and HFD mice (*SI Appendix*, Fig. S3 *B* and *C*). Accordingly, immunohistochemistry revealed a decrease of POMC and α-MSH production in the ARC of lean OX-A–injected, and obese vehicle-injected, mice. Also, this latter effect was reversed by SB334867 and AM251 (Fig. 2 *C*–*E* and *SI Appendix*, Fig. S3 *D* and *E*), as well by leptin, but only in *ob*/*ob* animals (*SI Appendix*, Fig. S3*E*) because of leptin resistance in the ARC of HFD mice (20). Biochemical analysis of the serum from a cohort of daily OX-A–injected lean mice revealed a reduction of α-MSH content (Fig. 2*F*) over 48 h of treatment with OX-A at doses ineffective on the average immobility-determined sleep profile (*SI Appendix*, Fig. S4 and Table S2). Notably, behavioral analysis of the same cohort of mice revealed a significant increase in food intake (Fig. 2*G*) and body weight (Fig. 2*H*). To confirm that OX-A–mediated reduction of POMC and of α-MSH production was due to an autocrine effect of 2-AG on CB_1R at the plasma membrane rather than at presynaptic or extra-ARC populations of CB_1Rs, we performed a thorough in vitro study in primary neurons from the ARC of either wild-type or POMC-eGFP lean mice. OX-A treatment halved the POMC expression and α-MSH release, in both types of primary neurons in a manner prevented by SB334867 or AM251 (*SI Appendix*, Figs. S5 *A*–*C* and S6*A*) (α-MSH levels in POMC-eGFP neurons: untreated: 90 ± 4.3; OX-A: 48.5 ± 5.2; OX-A plus SB334867: 85 ± 6.2; OX-A plus AM251: 80.5 ± 7.4; values are picograms per milliliter ± SEM). To exclude possible effects of OX-1R or CB_1R agonists/antagonists on the expression of the corresponding receptors, the mRNA levels of *Cnr1* or *Hcrtr1* were shown not to change in primary POMC-eGFP neurons after treatment with these agonists/antagonists (*SI Appendix*, Fig. S6 *C* and *D*). To provide further evidence that the effects of OX-A were due to CB_1R activation, experiments were performed in stabilized mHypoA-POMC/GFP cells transfected with CB_1 receptor-specific siRNA sequences (*SI Appendix*, Fig. S7*A*). We found a ∼50% decrease in CB_1R expression with respect to cells transfected with a scrambled siRNA control (*SI Appendix*, Fig. S7*B*), which in turn displayed levels of CB_1R expression identical to those observed in nontransfected cells. In CB_1R siRNA-transfected cells, OX-A inhibitory effects on both α-MSH production (*SI Appendix*, Fig. S7*A*) or POMC expression (*SI Appendix*, Fig. S7*C*) were greatly reduced, and this lack of effect was not modified by SB334867 or AM251 (*SI Appendix*, Fig. S7 *A* and *C*). Also, in mHypoA-POMC/GFP neurons, the levels of *Cnr1* or *Hcrtr1* mRNA did not change after treatment with the respective selective agonists (arachidonoyl-2-chloroethylamide or OX-A) or antagonists for the two receptors (*SI Appendix*, Fig. S7 *D* and *E*). Finally, to determine whether the pharmacological effects of AM251, OX-A, SB334867, and PD98059 were exerted directly on ARC (POMC) neurons or indirectly through other circuits, we compared them following either i.p. or intracerebroventricular stereotaxic injection in the third ventricle of lean and obese mice fed ad libitum. No significant difference was found between the two routes of administration concerning the effect on neuronal POMC expression, α-MSH production, ERK1/2-mediated $STAT3^{Ser727}$ or $STAT3^{Tyr705}$ phosphorylation, and *Pomc* mRNA levels (*SI Appendix*, Fig. S8).

OX-A and α-MSH Plasma Levels Are Inversely Correlated in Severe Human Obesity. Next, we explored whether higher levels of OX-A correlate with lower levels of α-MSH in subjects who exhibit clinical markers of obesity. Because a possible correlation between estrogen and plasma OX-A levels has been described in humans (28, 29), and a sex difference occurs in the POMC-driven regulation of energy expenditure and obesity in mice (30), we tested this hypothesis exclusively in male subjects ($n = 50$) who had suffered from obesity for at least 5 y in comparison with $n = 50$ male healthy, normal-weight, volunteers. Clinical, functional, and biochemical data were obtained from each patient at the baseline, and secondary causes of obesity were excluded. No subject was an alcohol abuser or under pharmacological treatment for any disease. Alanine aminotransferase (ALT) and γ-glutamyl transferase (GGT) enzymatic levels were measured by routine laboratory methods and resulted significantly higher in obese vs. nonobese men as a reliable hallmark of fatty liver disease associated with obesity. OX-A serum concentrations were significantly higher in obese vs. nonobese men (Fig. 3*A*). α-MSH serum concentrations were significantly lower in obese vs. nonobese men (Fig. 3*B*). Notably, a significant negative correlation was found between the circulating levels of OX-A and α-MSH ($r = -0.778$, $P < 0.05$) in obese subjects, whereas a weak positive correlation was found in healthy subjects ($r = 0.275$, $P > 0.05$) (Fig. 3*C*). In the serum of the same cohort of obese patients, negative correlations were also found between: (*i*) serum levels of α-MSH and both ALT ($r = -0.714$, $P < 0.05$) and GGT ($r = -0.828$, $P < 0.05$); (*ii*) α-MSH and body mass index (BMI) ($r = -0.425$, $P < 0.05$).

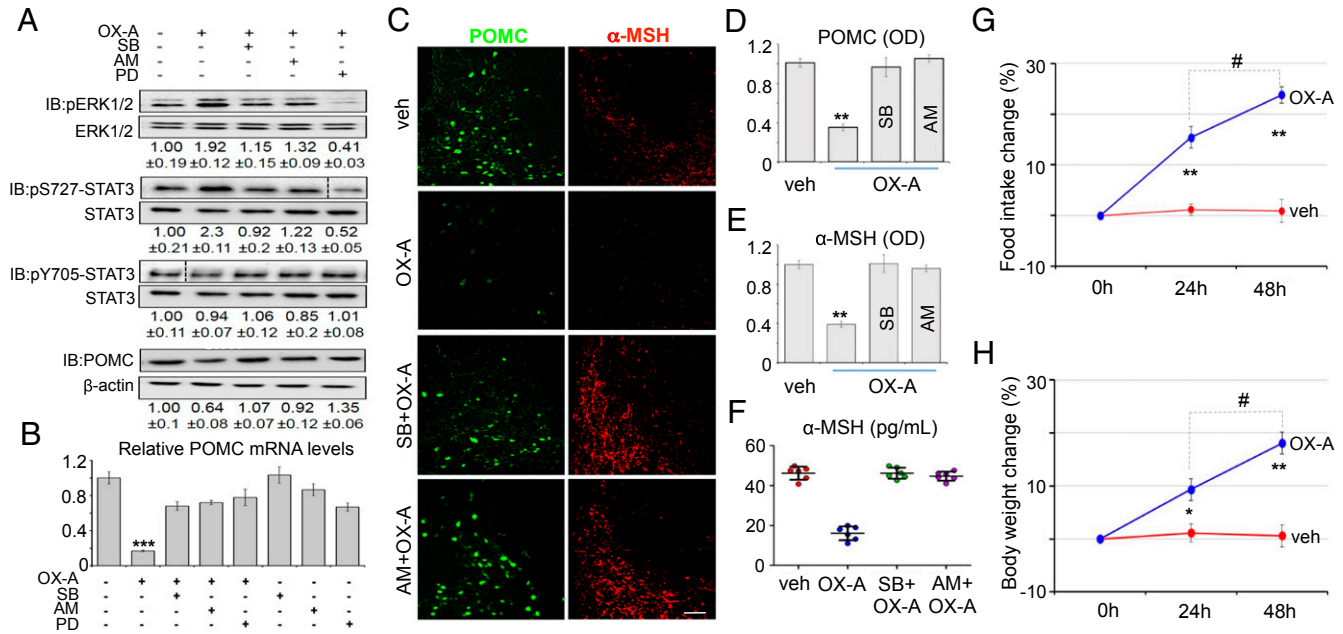

Fig. 2. OX-A reduces POMC and α-MSH expression by arresting *Pomc* gene transcription via the ERK1/2-pSTAT3^{Ser727} pathway, and causes overweight and hyperphagia. (*A*) Representative immunoblots of POMC, ERK1/2, and STAT3 expression in the ARC of vehicle- or OX-A–injected (i.p.) lean mice (6 h for POMC; 1 h for ERK1/2 or STAT3) pretreated (1 h) with either SB334867, AM251, or PD98059. Fold data represent the means ± SEM from $n = 3$ mice per group, normalized to the vehicle-treated group. Dashed lines indicate regions that were cropped. (*B*) POMC mRNA levels in lean mice normalized to the reference genes *Hprt* or *β-actin*; ***$P <$ 0.0005 vs. vehicle-injected mice. (*C*) POMC and α-MSH immunohistochemical expression in the ARC of vehicle-, OX-A-, SB334867-, or AM251-injected mice. (Scale bar: 100 μm for POMC and 200 μm for α-MSH.) (*D* and *E*) Optical density (OD, arbitrary units) of POMC or α-MSH immunoreactivity in lean mice. **$P < 0.005$ vs. vehicle-injected mice. Data are means ± SEM from $n = 300 \pm 30$ neurons per treatment. (*F*) Serum α-MSH levels of vehicle-, OX-A-, SB334867+OX-A-, AM251+OX-A–injected lean mice. (*G* and *H*) The 24- to 48-h OX-A injection increases food intake and body weight in lean mice. *$P < 0.05$ vs. 24-h vehicle-injected mice; **$P < 0.005$ vs. 24- or 48-h vehicle-injected mice; #$P < 0.05$ vs. 24-h OX-A–injected mice. Data are means ± SEM; $n = 6$ mice per group fed ad libitum. Statistical analysis was run by two-way ANOVA followed by the Bonferroni post hoc test.

Blocking OX-A Signaling Counteracts Overweight, Hyperphagia, and Alterations of Hepatosteatosis Markers Associated with Obesity in Mice. Adult male weight- and age-matched lean (WT and standard-fat diet fed) and obese mice (both *ob*/*ob* and HFD) were injected with SB334867 for 1 wk (30 mg/kg in lean mice and 60 mg/kg in obese mice, i.p.; $n = 2$ injections per d, 4 h before lights off and lights on, respectively) at doses ineffective on sleep duration (*SI Appendix*, Fig. S4*B* and Table S2). This treatment was able to reduce, in obese mice: (*i*) the circulating levels of ALT and GGT to lean control values (Fig. 4*A*); (*ii*) macrovesicular steatosis, this effect being more evident in HFD mice, which, after treatment, exhibited almost normal hepatic architecture and a strong reduction of macrovesicular lipid droplets, mainly around the portal tract, in comparison with livers from *ob*/*ob* SB334867-treated mice (Fig. 4*B*); (*iii*) hepatomegaly (Fig. 4*C*); (*iv*) food intake and body weight. In agreement with previous data (20), the percent food intake reduction by SB334867 was higher in *ob*/*ob* than HFD mice, whereas the percent weight reduction was higher in HFD than in *ob*/*ob* mice (Fig. 4*D*). A positive correlation was found between the change in body weight and ALT or GGT circulating levels in *ob*/*ob* ($r = 0.836$, $P < 0.05$ for ALT; $r = 0.886$, $P < 0.05$ for GGT) and HFD ($r = 0.873$, $P < 0.05$ for ALT; $r = 0.811$, $P < 0.05$ for GGT) mice, but not in lean mice ($r = 0.101$, $P > 0.05$ for ALT; $r = 0.482$, $P > 0.05$ for GGT). Notably, an elevation of circulating α-MSH to levels comparable to those of untreated lean mice was found in obese mice after SB334867 or AM251 treatment (Fig. 4*E*). Furthermore, a significant correlation was found between the SB334867-induced increase in α-MSH levels and the SB334867-induced decrease in the serum levels of ALT or GGT in the same cohorts of HDF ($r = 0.800$, $P < 0.05$ for ALT; $r = 0.859$, $P < 0.05$ for GGT) and *ob*/*ob* ($r = 0.803$, $P < 0.05$ for ALT; $r = 0.803$, $P < 0.05$ for GGT) mice after 1 wk of treatment with the antagonist. Taken together, these data establish, at least in mice, a cause–effect relationship between excessive OX-A levels, and the consequent impairment of α-MSH production, and some of the peripheral consequences of hyperphagia and obesity.

Discussion

The present study reveals the existence of a hypothalamic OX-1R/DAGLα/CB_1R loop through which OX-A controls POMC expression and α-MSH signaling in mice and, possibly, humans.

We report that OX-A–induced and CB_1R-mediated STAT3 phosphorylation at Ser-727 by ERK1/2 in lean mice affects negatively the expression of the *Pomc* gene, thus revealing an unprecedented endocannabinoid-mediated transcriptional mechanism through which long-term elevation of OX-A levels stimulates feeding in a satiety state. We provide evidence that such mechanism, by being under the negative control of leptin, may also contribute to obesity and some of its pathological consequences. Because a possible sex difference occurs in the regulation of plasma OX-A levels in humans (28,29,31) and in the POMC-driven regulation of energy expenditure and obesity in mice (30), we performed our study exclusively in male subjects. In particular, we show that OX-A acts via DAGLα-catalyzed biosynthesis of 2-AG, which then acts as an autocrine mediator on OX-1R/CB_1R-expressing POMC neurons of the ARC to inhibit STAT3 activity and subsequently repress POMC expression and the release of the anorectic peptide, α-MSH. These direct actions of OX-A were demonstrated in isolated primary POMC neurons and were shown to occur also in vivo in the ARC of lean mice, where they are enhanced during obesity, when OX-A/2-AG overactivity correlates with decreased α-MSH levels and increased BMI and hepatosteatosis. Accordingly, antagonism of OX-A action at OX-1R does not only counteract the impairment of POMC expression and α-MSH signaling, but,

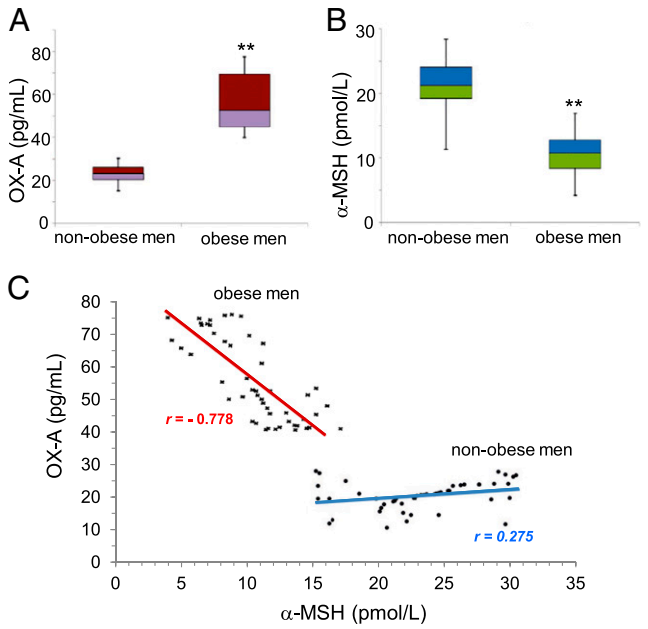

Fig. 3. OX-A and α-MSH levels in the serum of human obese patients are inversely correlated. (*A*) The serum median levels of OX-A in obese men are significantly higher than in nonobese men. Median: 50.75 pg/mL [25%, 75%: 20.45, 26.05] in the group of obese men; median: 23.3 pg/mL [25%, 75%: 42.82, 67.42] in nonobese men; mean ± SD = 55.0 ± 12.8 pg/mL in obese men; mean ± SD = 23.14 ± 4.4 pg/mL in nonobese men; $^{**}P < 0.001$ vs. nonobese men. (*B*) The serum median levels of α-MSH in obese men are significantly lower than in nonobese men. Median: 10.75 pmol/L [25%, 75%: 8.4, 12.77] in the group of obese men; median: 21.25 pmol/L [25%, 75%: 19.27, 24.07] in nonobese men; mean ± SD = 10.52 ± 3.05 pmol/L in obese men; mean ± SD = 20.93 ± 4.22 pmol/L in nonobese men; $^{**}P < 0.001$ vs. nonobese men. (*C*) The correlation between serum OX-A (in picograms per milliliter) and α-MSH (in picomoles per liter) levels is weak in nonobese men ($r = 0.275$) and significantly strong in obese men ($r = -0.778$). Data are from $n = 50$ male healthy normal weight (black dots) or obese (black asterisks) volunteers (mean age ± SD, 40.11 ± 2.48 y). The difference between the means of variables measured in obese and nonobese men was calculated by Mann–Whitney *U* test. Correlations were analyzed by using the Pearson test.

similarly to what has been found with CB_1R antagonists (32), also reduces hyperphagia, body weight, and steatosis in obese mice. The finding that OX-A modulates the function of CB_1R, for which it has no significant inherent affinity, by acting on the biosynthesis of its ligand provides yet another mechanism through which endocannabinoids, which affect food intake in a dual manner (33), exert hyperphagic actions at hypothalamic CB_1R. This finding is also relevant to the well-established inverse relationship between leptin and endocannabinoid signaling in obesity, anorexia, or inflammatory pain, which is also observed in humans (34, 35). Indeed, hypothalamic 2-AG levels increase significantly in models of genetic [*ob*/*ob* and *db*/*db* mice (2)] or diet-induced (20) leptin signaling deficiency and obesity, where a significant increase of OX-A signaling to many target areas, including the ARC, is also observed (7, 20). In the present study, by reproducing the effect of leptin deficiency on OX-A levels through the administration of the exogenous neuropeptide, we provide direct biochemical in vivo evidence for the occurrence of a stimulatory effect of OX-1R activation on 2-AG biosynthesis in POMC neurons. In lean animals, OX-A–induced elevation of endocannabinoid tone, and the subsequent reduction of α-MSH levels, may represent a physiological mechanism ensuring that OX-A–induced alertness is accompanied by food seeking (17). Accordingly to this physiological function, the OX-A levels measured in brain dialysates or CSF of rodents peak late in the active period (36, 37) and, possibly, exhibit a robust time-dependent fluctuation of the intracellular processing of the prepropeptide, and/or transport and release of the peptide from the somata in the LH to fibers and terminals in the ARC. During obesity, however, the aberrant activation of OX-A–mediated endocannabinoid signaling at POMC neurons, triggered by deficits in leptin signaling, creates a vicious circle leading to inhibition of POMC synthesis, hyperphagia, additional body weight gain, and hepatosteatosis, as documented by the present findings. Indeed, the increase in body weight described in OX-A–deficient mice could be attributed to physical hypoactivity during the light and dark phases rather than overeating or overdrinking (38). Here, we show that long-term OX-A overactivity due to lack of leptin signaling contributes to obesity instead via endocannabinoid-mediated suppression of POMC expression and hyperphagia, because the selective OX-1R antagonist SB334867 reduced body weight and food intake at doses ineffective on sleep duration and locomotion. Similarly to what was found in the periaqueductal gray (7) or in other LH target areas (20), also in the ARC of *ob*/*ob* and HFD-fed mice we found the increase of OX-A trafficking and release to terminals as well as the compensatory reduction or no change in the levels of prepro-OX and OX-A in the LH (20, 39). The present discovery of an orexin/endocannabinoid/melanocortin interaction, and its impact on hyperphagia, obesity, and fatty liver, calls for investigations on potential synergies between OX-1R antagonists and/or CB_1R antagonists and/or MC4R agonists, aiming at counteracting eating disorders such as binge eating, but also obesity and

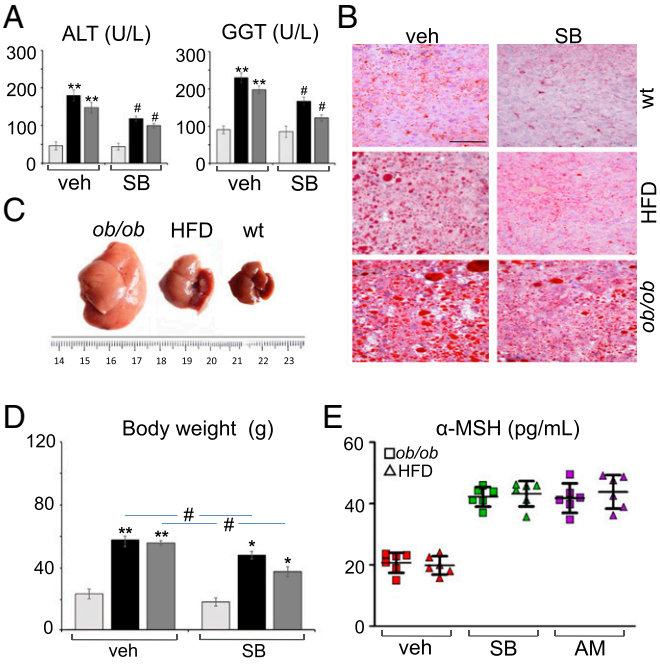

Fig. 4. SB334867 treatment counteracts elevation of circulating hepatic injury markers and reduction of α-MSH levels associated with steatosis and obesity. (*A*) SB334867 injection reduces serum ALT and GGT levels (lean, light gray bars; *ob*/*ob*, black bars; HFD, dark gray bars) in obese mice. $^{**}P < 0.005$ vs. vehicle-injected lean mice; $^{\#}P < 0.05$ vs. SB334867-injected lean mice. (*B*) SB334867 injection reduces both size and number of lipid droplets in obese livers as detected by Oil Red staining. (Scale bar: 60 μm.) (*C*) Hepatomegaly and pale yellow discoloring in obese mice. (*D*) SB334867 injection reduces body weight (lean, light gray bars; *ob*/*ob*, black bars; HFD, dark gray bars) in obese mice. $^{**}P < 0.005$ vs. vehicle-injected lean mice; $^{*}P < 0.05$ vs. SB334867-injected lean mice; $^{\#}P < 0.05$ vs. vehicle-injected *ob*/*ob* or HFD mice. (*E*) SB334867 or AM251 injection increases serum α-MSH levels in obese mice. Data are means ± SEM; $n = 6$ mice per group fed ad libitum. Statistical analysis was run by two-way ANOVA followed by the Bonferroni post hoc test.

CELL BIOLOGY

dysmetabolism, with new safe and effective polypharmacological or multitarget approaches (40).

Materials and Methods

Animals. Experiments were performed under institutional approval of the Second University of Naples and according to the guidelines of the institutional ethical code and the Italian (Decrete Law 116/92) and European (Official Journal of European Community L358/1 December 18, 1986) regulations for the care and use of laboratory animals.

Immunohistochemistry. Under deep pentobarbital anesthesia, the mice were perfused transcardially. Brains were cut into 10-μm-thick serial sections in the coronal plane and processed for immunofluorescence or immunoperoxidase with specific primary antibodies (see *SI Appendix* for details).

Lipid Extraction and 2-AG Measurement. Mice were killed by cervical dislocation, the brains removed, and the ARC rapidly dissected. Tissue samples were pooled and analyzed using liquid chromatography–atmospheric pressure chemical ionization–mass spectrometry as detailed in *SI Appendix*.

α-MSH and OX-A Measurements. Serum α-MSH or CSF OX-A levels were determined using a commercial ELISA kit according to the manufacturer's instructions (see *SI Appendix* for details).

***Pomc* mRNA Quantification.** *Pomc* mRNA was quantified by RT-PCR analysis using the primers designed by Allele-Id software, version 7.0 (Biosoft International), and synthesized (HPLC-purification grade) by MWG-Biotech (see *SI Appendix* for details).

Study Population and Hormone Measurements. The study was approved by the Ethics Committee of the Faculty of Medicine, University of Naples Federico II (authorization no. 193/06, October 25, 2006; amendment no. 193/06/ESES1, October 1, 2014), and informed consent was obtained from the subjects. The study was performed on $n = 50$ unrelated white young male adults who had suffered from obesity for at least 5 y. All of the data were compared with that obtained from 50 male healthy, normal-weight volunteers. Circulating α-MSH or OX-A levels were measured using an ultrasensitive fluorescent enzyme immunoassay or an RIA kit, respectively (see *SI Appendix* for details).

Supplemental methods, along with any additional supplemental data, are available in *SI Appendix*; references unique to this section appear only in *SI Appendix*.

ACKNOWLEDGMENTS. We are very grateful to Prof. Ken Mackie (Indiana University), who kindly provided the DAGLα antibody; and Roman Polishchuk and the staff of the Advanced Microscopy and Imaging Core of the TIGEM for their technical support in TEM and confocal microscopy. We are very grateful to Pasquale Barba (Institute of Protein Biochemistry of CNR) for the technical support at the IGB–IBP FACS Facility.

1. Flores A, Maldonado R, Berrendero F (2013) Cannabinoid-hypocretin cross-talk in the central nervous system: What we know so far. *Front Neurosci* 7:256.
2. Di Marzo V, et al. (2001) Leptin-regulated endocannabinoids are involved in maintaining food intake. *Nature* 410(6830):822–825.
3. Di Marzo V (2011) Endocannabinoids: An appetite for fat. *Proc Natl Acad Sci USA* 108(31):12567–12568.
4. Sakurai T (2014) Roles of orexins in the regulation of body weight homeostasis. *Obes Res Clin Pract* 8(5):e414–e420.
5. Turunen PM, Jäntti MH, Kukkonen JP (2012) OX1 orexin/hypocretin receptor signaling through arachidonic acid and endocannabinoid release. *Mol Pharmacol* 82(2): 156–167.
6. Ho J, Cox JM, Wagner EJ (2007) Cannabinoid-induced hyperphagia: Correlation with inhibition of proopiomelanocortin neurons? *Physiol Behav* 92(3):507–519.
7. Cristino L, et al. (2016) Orexin-A and endocannabinoid activation of the descending antinociceptive pathway underlies altered pain perception in leptin signaling deficiency. *Neuropsychopharmacology* 41(2):508–520.
8. Schwartz MW, Woods SC, Porte D, Jr, Seeley RJ, Baskin DG (2000) Central nervous system control of food intake. *Nature* 404(6778):661–671.
9. Cone RD (2005) Anatomy and regulation of the central melanocortin system. *Nat Neurosci* 8(5):571–578.
10. Elias CF, et al. (1998) Chemically defined projections linking the mediobasal hypothalamus and the lateral hypothalamic area. *J Comp Neurol* 402(4):442–459.
11. Yaswen L, Diehl N, Brennan MB, Hochgeschwender U (1999) Obesity in the mouse model of pro-opiomelanocortin deficiency responds to peripheral melanocortin. *Nat Med* 5(9):1066–1070.
12. Balthasar N, et al. (2004) Leptin receptor signaling in POMC neurons is required for normal body weight homeostasis. *Neuron* 42(6):983–991.
13. Cone RD (2000) Haploinsufficiency of the melanocortin-4 receptor: Part of a thrifty genotype? *J Clin Invest* 106(2):185–187.
14. Ma X, Zubcevic L, Brüning JC, Ashcroft FM, Burdakov D (2007) Electrical inhibition of identified anorexigenic POMC neurons by orexin/hypocretin. *J Neurosci* 27(7): 1529–1533.
15. Chemelli RM, et al. (1999) Narcolepsy in orexin knockout mice: Molecular genetics of sleep regulation. *Cell* 98(4):437–451.
16. Kiyashchenko LI, et al. (2002) Release of hypocretin (orexin) during waking and sleep states. *J Neurosci* 22(13):5282–5286.
17. López M, et al. (2007) Orexin expression is regulated by alpha-melanocyte-stimulating hormone. *J Neuroendocrinol* 19(9):703–707.
18. Koch M, et al. (2015) Hypothalamic POMC neurons promote cannabinoid-induced feeding. *Nature* 519(7541):45–50.
19. Crespo I, Gómez de Heras R, Rodríguez de Fonseca F, Navarro M (2008) Pretreatment with subeffective doses of rimonabant attenuates orexigenic actions of orexin A-hypocretin 1. *Neuropharmacology* 54(1):219–225.
20. Cristino L, et al. (2013) Obesity-driven synaptic remodeling affects endocannabinoid control of orexinergic neurons. *Proc Natl Acad Sci USA* 110(24):E2229–E2238.
21. Hentges ST (2007) Synaptic regulation of proopiomelanocortin neurons can occur distal to the arcuate nucleus. *J Neurophysiol* 97(5):3298–3304.
22. Bénard G, et al. (2012) Mitochondrial CB_1 receptors regulate neuronal energy metabolism. *Nat Neurosci* 15(4):558–564.
23. Bouaboula M, et al. (1995) Activation of mitogen-activated protein kinases by stimulation of the central cannabinoid receptor CB1. *Biochem J* 312(Pt 2):637–641.
24. Ammoun S, Lindholm D, Wootz H, Akerman KE, Kukkonen JP (2006) G-protein-coupled OX1 orexin/hcrtr-1 hypocretin receptors induce caspase-dependent and -independent cell death through p38 mitogen-/stress-activated protein kinase. *J Biol Chem* 281(2):834–842.
25. Kano M, Ohno-Shosaku T, Hashimotodani Y, Uchigashima M, Watanabe M (2009) Endocannabinoid-mediated control of synaptic transmission. *Physiol Rev* 89(1): 309–380.
26. Chen Z, et al. (2001) MAP kinases. *Chem Rev* 101(8):2449–2476.
27. Kyosseva SV (2004) Mitogen-activated protein kinase signaling. *Int Rev Neurobiol* 59:201–220.
28. El-Sedeek MSh, Korish AA, Deef MM (2010) Plasma orexin-A levels in postmenopausal women: Possible interaction with estrogen and correlation with cardiovascular risk status. *BJOG* 117(4):488–492.
29. Messina G, et al. (2013) Hormonal changes in menopause and orexin-A action. *Obstet Gynecol Int* 2013:209812.
30. Burke LK, et al. (2016) Sex difference in physical activity, energy expenditure and obesity driven by a subpopulation of hypothalamic POMC neurons. *Mol Metab* 5(3): 245–252.
31. Baranowska B, Wolińska-Witort E, Martyńska L, Chmielowska M, Baranowska-Bik A (2005) Plasma orexin A, orexin B, leptin, neuropeptide Y (NPY) and insulin in obese women. *Neuroendocrinol Lett* 26(4):293–296.
32. Tam J, et al. (2012) Peripheral cannabinoid-1 receptor inverse agonism reduces obesity by reversing leptin resistance. *Cell Metab* 16(2):167–179.
33. Bellocchio L, et al. (2010) Bimodal control of stimulated food intake by the endocannabinoid system. *Nat Neurosci* 13(3):281–283.
34. Monteleone P, et al. (2005) Blood levels of the endocannabinoid anandamide are increased in anorexia nervosa and in binge-eating disorder, but not in bulimia nervosa. *Neuropsychopharmacology* 30(6):1216–1221.
35. Nicholson J, et al. (2015) Leptin levels are negatively correlated with 2-arachidonoylglycerol in the cerebrospinal fluid of patients with osteoarthritis. *PLoS One* 10(4):e0123132.
36. Yoshida Y, et al. (2001) Fluctuation of extracellular hypocretin-1 (orexin A) levels in the rat in relation to the light-dark cycle and sleep-wake activities. *Eur J Neurosci* 14(7):1075–1081.
37. Fujiki N, et al. (2001) Changes in CSF hypocretin-1 (orexin A) levels in rats across 24 hours and in response to food deprivation. *Neuroreport* 12(5):993–997.
38. Tabuchi S, et al. (2014) Conditional ablation of orexin/hypocretin neurons: A new mouse model for the study of narcolepsy and orexin system function. *J Neurosci* 34(19):6495–6509.
39. Nobunaga M, et al. (2014) High fat diet induces specific pathological changes in hypothalamic orexin neurons in mice. *Neurochem Int* 78:61–66.
40. Kälin S, et al. (2015) Hypothalamic innate immune reaction in obesity. *Nat Rev Endocrinol* 11(6):339–351.